

$K_L^0 p \rightarrow p K_S^0$  BACKWARD SCATTERING FROM 1.0 TO 7.5 GeV/c \*

G. W. Brandenburg, W. B. Johnson, D.W.G.S. Leith, J. S. Loos,\*\*  
G. J. Luste,\*\*\* J.A.J. Matthews, K. Moriyasu,† W. M. Smart,††  
F. C. Winkelmann,††† and R. J. Yamartino‡

Stanford Linear Accelerator Center  
Stanford University, Stanford, California 94305

ABSTRACT

Backward scattering in the reaction  $K_L^0 p \rightarrow p K_S^0$  is studied in the momentum interval 1.0 to 7.5 GeV/c. Comparison of  $K_L^0 p \rightarrow p K_S^0$  and  $K^+ p \rightarrow p K^+$  backward scattering, where respectively  $\Sigma$  exchange and  $\Lambda$  plus  $\Sigma$  exchange can contribute in the u channel, reveals that

$$\left(\frac{d\sigma}{d\Omega}\right)_{180^\circ}(K_L^0 p \rightarrow p K_S^0) \ll \left(\frac{d\sigma}{d\Omega}\right)_{180^\circ}(K^+ p \rightarrow p K^+)$$

above the resonance region. This result provides direct evidence for the dominance of the  $\Lambda$  contribution over the  $\Sigma$  contribution in the  $K^+ p \rightarrow p K^+$  production amplitude.

(Submitted to Phys. Rev. Letters.)

---

\*Work supported by the U. S. Atomic Energy Commission.

\*\*Now at Duke University, Durham, North Carolina.

\*\*\*Now at University of Toronto, Toronto, Canada.

†Now at University of Washington, Seattle, Washington.

††Now at National Accelerator Laboratory, Batavia, Illinois.

†††Now at Lawrence Berkeley Laboratory, Berkeley, California.

‡Now at Purdue University, Lafayette, Indiana.

In this Letter we present the first measurement of the backward differential cross section for the reaction

$$K_L^0 p \rightarrow p K_S^0 \quad (1)$$

in the momentum interval 1.0 to 7.5 GeV/c. When combined with previously measured  $K^+ p \rightarrow p K^+$  cross sections, these data provide a direct comparison of  $\Lambda$  and  $\Sigma$  exchange couplings.

Indirect comparisons of the  $\Lambda$  and  $\Sigma$  couplings have been made using backward  $\pi^- p \rightarrow \Lambda^0 K^0$  data<sup>1,2</sup> which, like reaction (1), isolates u-channel  $\Sigma$  exchange. However, comparisons of the reactions  $K^+ p \rightarrow p K^+$  and  $\pi^- p \rightarrow \Lambda^0 K^0$  involve systematic uncertainties from the use of SU(3) relations,<sup>2</sup> and from kinematic effects when particle masses in the initial and final states are different.<sup>3</sup>

Our results are based on the analysis of  $\sim 1$  million photographs of  $K_L^0 p$  interactions in the SLAC 40-inch hydrogen bubble chamber. The data in reaction (1) were found in a scan of one-prong-plus-vee events, measured on conventional film plane machines, and processed with the TVGP-SQUAW computer programs. The incident flux and momentum spectrum were determined by measuring  $K_L^0$  decays in the chamber, as described in Ref. 4.

The total sample for all center-of-mass scattering angles ( $-1 < \cos \theta < 1$ ) consists of 2411 events. In the backward hemisphere ( $\cos \theta < 0$ ) there are 425 events, none of which are kinematically ambiguous with other hypotheses. A special scan of 15% of the film for backward  $K_L^0 p \rightarrow p K_S^0$  events yields a scanning efficiency of 70% for  $\theta_{LAB} > 45^\circ$ ,<sup>5</sup> compared to the scanning efficiency of 90% for forward events. The scanning efficiency for backward events is found to be independent of beam momentum and of  $K_S^0$  decay length for lengths above 0.30 cm. In addition to the scanning efficiency correction, events have been corrected for the neutral decay mode of the  $K_S^0$ , for  $K_S^0$  decay loss (average correction factor 1.08 for  $\cos \theta < 0$ ),

and for loss of events with steeply dipping protons (correction factor 1.05). The uncertainties in our data points include their statistical error as well as the uncertainties in the scanning efficiency, the beam momentum spectrum and the correction for loss of events with steeply dipping protons. However, an overall systematic uncertainty in the magnitude of the  $K_L^0$  flux,  $\sim 10\%$ ,<sup>4</sup> has not been included.

The differential cross sections for reaction (1) are presented in Fig. 1 for six momentum intervals spanning our energy range. The general features of these angular distributions are the well defined forward and backward peaks occurring in all the data, the existence of a shoulder at  $\cos \theta \sim 0.6 - 0.8$  which disappears with increasing momentum, and the very rapid decrease of the  $90^\circ$  cross section with energy.<sup>6</sup> The forward cross sections have been discussed previously.<sup>7</sup>

We now consider the backward peak in the  $K_L^0 p \rightarrow p K_S^0$  differential cross section. To obtain backward cross sections, the data are extrapolated to  $180^\circ$  ( $u'=0$ ) assuming an exponential form<sup>8</sup>:

$$\frac{d\sigma}{du'} = \left( \frac{d\sigma}{du'} \right)_0 e^{-bu'} = \frac{\pi}{k^2} \left( \frac{d\sigma}{d\Omega} \right)_{180^\circ} e^{-bu'} \quad (2)$$

where  $u' = u_{\max} - u$ . The fitted slope parameters, the resulting backward cross sections, and the momentum transfer intervals used for the extrapolation are recorded in Table I. The backward cross section errors are taken to be the fractional uncertainty in the last data point.

For the highest momentum interval, 5 - 7.5 GeV/c, the data are insufficient to determine the backward slope. In this instance, the slope parameter in Eq. (2) is fixed to the high energy value,  $b = 5.5 \pm 0.5 \text{ GeV}^{-2}$ ,<sup>1</sup> for the related reaction  $\pi^- p \rightarrow \Lambda^0 K^0$ .<sup>9</sup> This value is in good agreement with the average slope from reaction (1) below 5 GeV/c, although the backward slopes in the  $K_L^0 p \rightarrow p K_S^0$  data do vary significantly in the resonance region.

The backward cross sections for reaction (1) are plotted as a function of  $K_L^0$  momentum in Fig. 2. For comparison, Fig. 2 also shows  $(d\sigma/d\Omega)_{180^\circ}$  for the reactions  $K^+p \rightarrow pK^+$ ,<sup>10</sup>  $K^-p \rightarrow pK^-$ ,<sup>11</sup> and  $K^+n \rightarrow nK^+$ .<sup>12</sup> For the  $K^+n$  reaction the cross section has been reduced by a factor of four to correspond to the  $K^0p \rightarrow pK^0$  contribution to  $K_L^0p \rightarrow pK_S^0$ . Although the  $K^+p \rightarrow pK^+$ ,  $K^-p \rightarrow pK^-$  and  $K_L^0p \rightarrow pK_S^0$  backward cross sections are approximately equal for momenta near 1.5 GeV/c, it is observed that they diverge rapidly above 2 GeV/c so that for momenta  $\gtrsim 3$  GeV/c

$$\left(\frac{d\sigma}{d\Omega}\right)_{180^\circ}(K_L^0p \rightarrow pK_S^0) \approx \frac{1}{5} \left(\frac{d\sigma}{d\Omega}\right)_{180^\circ}(K^+p \rightarrow pK^+) \quad (3a)$$

$$\left(\frac{d\sigma}{d\Omega}\right)_{180^\circ}(K_L^0p \rightarrow pK_S^0) \approx 5 \left(\frac{d\sigma}{d\Omega}\right)_{180^\circ}(K^-p \rightarrow pK^-) \quad (3b)$$

A similar result has recently been reported at 2.3 GeV/c in the annihilation channel  $\bar{p}p \rightarrow \bar{K}K$ ,<sup>13</sup> where the ratio of cross sections is  $\sigma(\bar{p}p \rightarrow K_S^0K_L^0)/\sigma(\bar{p}p \rightarrow K^-K^+) = 0.1 \pm 0.06$  in agreement with Eq. (3a).

To determine the energy dependence of the relations in Eq. (3), the backward cross sections in Fig. 2 are parameterized by the power law form  $(d\sigma/d\Omega)_{180^\circ} \propto P_{LAB}^{-n}$  for momenta  $\gtrsim 2.5$  GeV/c. For  $K^+p$  and  $K^-p$  reactions we find  $n \sim 2.7$  and  $n \sim 3.6$  respectively, as shown by the curves in Fig. 2. In the analysis of the  $K_L^0p \rightarrow pK_S^0$  data, we assume that the  $K^0p \rightarrow pK^0$  amplitude dominates the  $\bar{K}^0p \rightarrow p\bar{K}^0$  amplitude above  $\sim 2.5$  GeV/c. The  $K^+n \rightarrow nK^+$  data at 2 GeV/c are combined therefore with the  $K_L^0p \rightarrow pK_S^0$  data, yielding the value  $n = 2.5 \pm 0.8$ ,<sup>14</sup> in agreement with the backward  $K^+p \rightarrow pK^+$  data and consistent with no energy dependence for the result in Eq. (3a).

The comparatively rapid falloff of  $(d\sigma/d\Omega)_{180^\circ}(K^-p \rightarrow pK^-)$  with energy can be understood by noting that exotic ( $Z^*$ ) exchange or double Regge exchange is required above the direct channel resonance region.<sup>15</sup> Duality then predicts a similar

behavior for the resonance region where cancellations must occur in the backward direction between the amplitudes for different s-channel resonances.

The smallness of backward  $K_L^0 p \rightarrow pK_S^0$  compared to  $K^+ p \rightarrow pK^+$  has a direct interpretation in terms of  $\Lambda$  and  $\Sigma$  trajectory exchange. Backward  $K_L^0 p \rightarrow pK_S^0$  may proceed via  $\Sigma$  exchange, whereas backward  $K^+ p$  scattering may proceed via exchange of  $\Sigma$  or  $\Lambda$ . Since the  $\Sigma$ -exchange contribution to both reactions is identical, the  $\Lambda$ -exchange contribution to  $K^+ p \rightarrow pK^+$  must dominate, even though  $\Sigma_\delta$  is the highest lying hyperon trajectory that can contribute in this channel.

We note that this result is consistent with a prediction of Barger<sup>16</sup> that  $\Lambda_\alpha, \Lambda_\gamma$  should dominate both  $\Sigma_\alpha, \Sigma_\gamma$  and  $\Sigma_\beta, \Sigma_\delta$  contributions to  $K^+ p \rightarrow pK^+$  backward scattering.<sup>17</sup> Support for this argument comes from dispersion relation calculations that find  $g_{\Lambda\bar{K}N}^2 \gg g_{\Sigma\bar{K}N}^2$  from low energy data,<sup>18</sup> and also from SU(3) models<sup>16</sup> that relate  $N_\alpha$  and  $\Delta_\delta$  Regge amplitudes in  $\pi^\pm p$  backward scattering<sup>19</sup> to the  $\Lambda$  and  $\Sigma$  amplitudes in backward  $K^+ p \rightarrow pK^+$  production.

In conclusion, the comparison of backward  $K_L^0 p \rightarrow pK_S^0$  and  $K^+ p \rightarrow pK^+$  cross sections provides evidence that u-channel  $\Lambda$  exchange dominates  $\Sigma$  exchange in the high energy  $K^+ p \rightarrow pK^+$  production amplitude.

We wish to acknowledge the assistance provided by R. Watt and the crew of the SLAC 40-inch bubble chamber, by J. Brown and the scanning and measuring staff at SLAC, and by D. Johnson for data handling.

## REFERENCES

1. W. Beusch et al., Nucl. Phys. B19, 546 (1970); M. Pepin et al., Phys. Letters 26B, 35 (1967); D. J. Crennell et al., Phys. Rev. D6, 1220 (1972); O. I. Dahl et al., Phys. Rev. 163, 1430 (1967).
2. B. Kayser, NAL Report No. NAL-THY-73 (1972); B. Kayser and F. Hayot, Phys. Rev. D (to be published).
3. G. H. Trilling, Nucl. Phys. B40, 13 (1972); R. Barloutaud et al., Nucl. Phys. B26, 557 (1971).
4. G. W. Brandenburg et al., SLAC Report No. SLAC-PUB-1084 (1972).
5. Statistical errors dominate systematic uncertainties in the scanning efficiency for the events with  $\theta_{\text{LAB}} > 45^\circ$ . Systematic errors therefore make only a small contribution to the final uncertainty in the backward cross sections.
6. G. W. Brandenburg et al., to be published.
7. A. D. Brody et al., Phys. Rev. Letters 26, 1050 (1971).
8. The  $K_L^0 p \rightarrow p K_S^0$  backward differential cross section is in good agreement with a single exponential for  $u' \lesssim 0.3 \text{ GeV}^2$ , for the low energy data, and for  $u' \lesssim 0.6 \text{ GeV}^2$ , for data above  $\sim 3 \text{ GeV}/c$ . This result is in agreement with backward  $\pi^- p \rightarrow \Lambda^0 K^0$  data, which also isolates u-channel  $\Sigma$  exchange, see Ref. 1.
9. Using the  $\pi^- p \rightarrow \Lambda^0 K^0$  slope to evaluate the backward cross sections in the momentum intervals 2 - 2.5, 2.5 - 3.5 and 3.5 - 5.0 GeV/c, we obtain the values,  $(d\sigma/du')_0 = 247 \pm 59 \mu\text{b}/\text{GeV}^2$ ,  $36.7 \pm \frac{17.7}{11.0} \mu\text{b}/\text{GeV}^2$  and  $7.3 \pm \frac{6.1}{3.7} \mu\text{b}/\text{GeV}^2$  respectively. For comparison see Table I.
10. A. S. Carroll et al., Phys. Rev. Letters 21, 1282 (1968) (1.04, 1.12, 1.20, 1.30, 1.40, 1.49, 1.61, 1.66, 1.71, 1.79, 1.88, 2.00, 2.07, 2.20, 2.33, and 2.45 GeV/c);  
J. Whitmore et al., Phys. Rev. D3, 1092 (1971) (2.53, 2.76, 3.20 GeV/c);

- J. Banaigs et al., Nucl. Phys. B9, 640 (1969) (3.55 GeV/c);
- V. Chabaud et al., Phys. Letters 38B, 445 (1972) (5.0 GeV/c);
- W. F. Baker et al., Phys. Letters B28, 291 (1968) (5.2 and 6.9 GeV/c).
11. A. S. Carroll et al., Phys. Rev. Letters 23, 887 (1969) (1.20, 1.39, 1.49, 1.60, 1.71, 1.80, 1.96, 2.18, and 2.44 GeV/c);
- J. Banaigs et al. (see Ref. 10);
- V. Chabaud et al. (see Ref. 10);
- W. R. Holley et al., Phys. Rev. 154, 1273 (1967) (1.30 GeV/c);
- C. Daum et al., Nucl. Phys. B6, 273 (1968) (1.43, 1.53 GeV/c);
- N. M. Gelfand et al., Phys. Rev. Letters 17, 1224 (1966) (1.10, 1.18 GeV/c).
12. D. W. Davies et al., Phys. Rev. D5, 1 (1972); D. W. Davies, private communication.
13. T. Fields et al., Phys. Letters 40B, 503 (1972).
14. A similar energy dependence is found for the backward  $\pi^- p \rightarrow \Lambda^0 K^0$  reaction, Ref. 1, where  $n = 2.2 \pm 0.3$  for data above  $\sim 4$  GeV/c.
15. C. Michael, Phys. Letters 29B, 230 (1969).
16. V. Barger, Phys. Rev. 179, 1371 (1969).
17. Other points of view also exist, see Ref. 2 and C. Schmid and J. K. Storrow, Nucl. Phys. B44, 269 (1972).
18. J. K. Kim, Phys. Rev. Letters 19, 1079 (1967);
- R. Levi-Setti, Proc. Lund Int'l. Conf. on Elementary Particles (Berlingska Boktryckeriet, Lund, Sweden, 1969).
19. V. Barger and D. Cline, Phys. Rev. Letters 21, 392 (1968).

TABLE I

 $K_L^0 p \rightarrow p K_S^0$  Backward Differential Cross Sections at  $180^\circ$  ( $u = u_{\max}$ )

Beam Momentum (GeV/c)	Momentum Transfer Interval, $u'$ (GeV <sup>2</sup> )	Slope (GeV <sup>-2</sup> )	$\left(\frac{d\sigma}{du}\right)_{u=u_{\max}}$ ( $\mu\text{b}/\text{GeV}^2$ )	$\left(\frac{d\sigma}{d\Omega}\right)_{180^\circ}$ ( $\mu\text{b}/\text{sr}$ )
1.0 - 1.5	0.0 - 0.2 <sup>(b)</sup>	$7.5 \pm 1.8$	$2750 \pm 600$	$330 \pm 75$
1.5 - 2.0	0.0 - 0.3	$6.0 \pm 1.5$	$730 \pm 170$	$138 \pm 32$
2.0 - 2.5	0.0 - 0.4	$9.0 \pm 2.0$	$350 \pm 120$	$90 \pm 30$
2.5 - 3.5	0.0 - 0.6	$1.5 \pm 1.4$	$17 \pm 7.4$	$6.2 \pm 2.7$
3.5 - 5.0	0.0 - 0.8	$6.0 \pm 3.0$	$7.7 \pm \begin{matrix} 6.4 \\ 3.8 \end{matrix}$	$4.4 \pm \begin{matrix} 3.6 \\ 2.2 \end{matrix}$
5.0 - 7.5	0.0 - 0.6	$5.5 \pm 0.5$ <sup>(a)</sup>	$1.3 \pm \begin{matrix} 2.9 \\ 1.0 \end{matrix}$	$1.1 \pm \begin{matrix} 2.6 \\ 0.9 \end{matrix}$

<sup>(a)</sup> Slope value taken from the related reaction  $\pi^- p \rightarrow \Lambda^0 K^0$  (see text).

<sup>(b)</sup> Data intervals chosen consistent with the backward differential cross section being described by a single exponential, as in Eq. (2).



## LIST OF FIGURES

1. Differential cross section for  $K_L^0 p \rightarrow K_S^0 p$  plotted in six momentum intervals between 1.0 and 7.5 GeV/c. The uncertainties on the points are calculated as discussed in the text. The data point between  $0.5 \geq \cos \theta \geq -0.5$  in the 5 - 7.5 GeV/c data represents an upper bound on this cross section corresponding to 1.9 events (85% confidence level) when no events were seen.
2. Backward differential cross sections,  $(d\sigma/d\Omega)_{180^\circ}$ , for  $(\bullet) K_L^0 p \rightarrow p K_S^0$ ,  $(\blacksquare) K^+ n \rightarrow n K^+$ ,  $(\square) K^+ p \rightarrow p K^+$ , and  $(\diamond) K^- p \rightarrow p K^-$  plotted as a function of momentum. The curves on the data are of the form  $(d\sigma/d\Omega)_{180^\circ} \sim P_{LAB}^{-n}$ . The  $K^+ n \rightarrow n K^+$  cross section has been divided by four to facilitate comparison with the  $K_L^0 p \rightarrow p K_S^0$  data (see text).

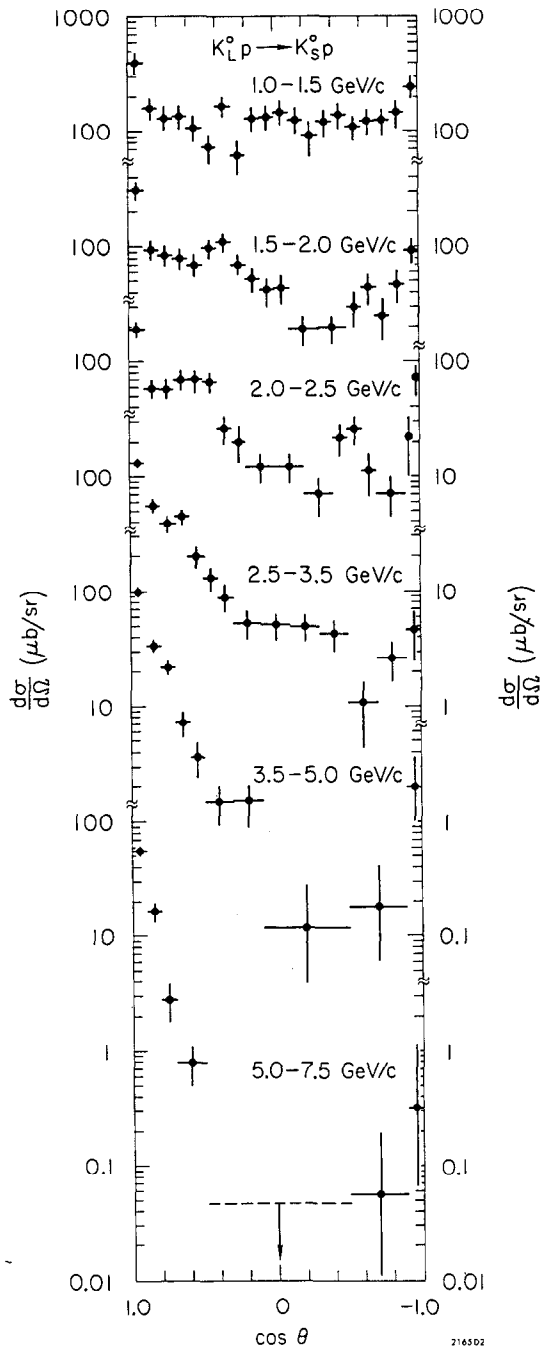


Fig. 1

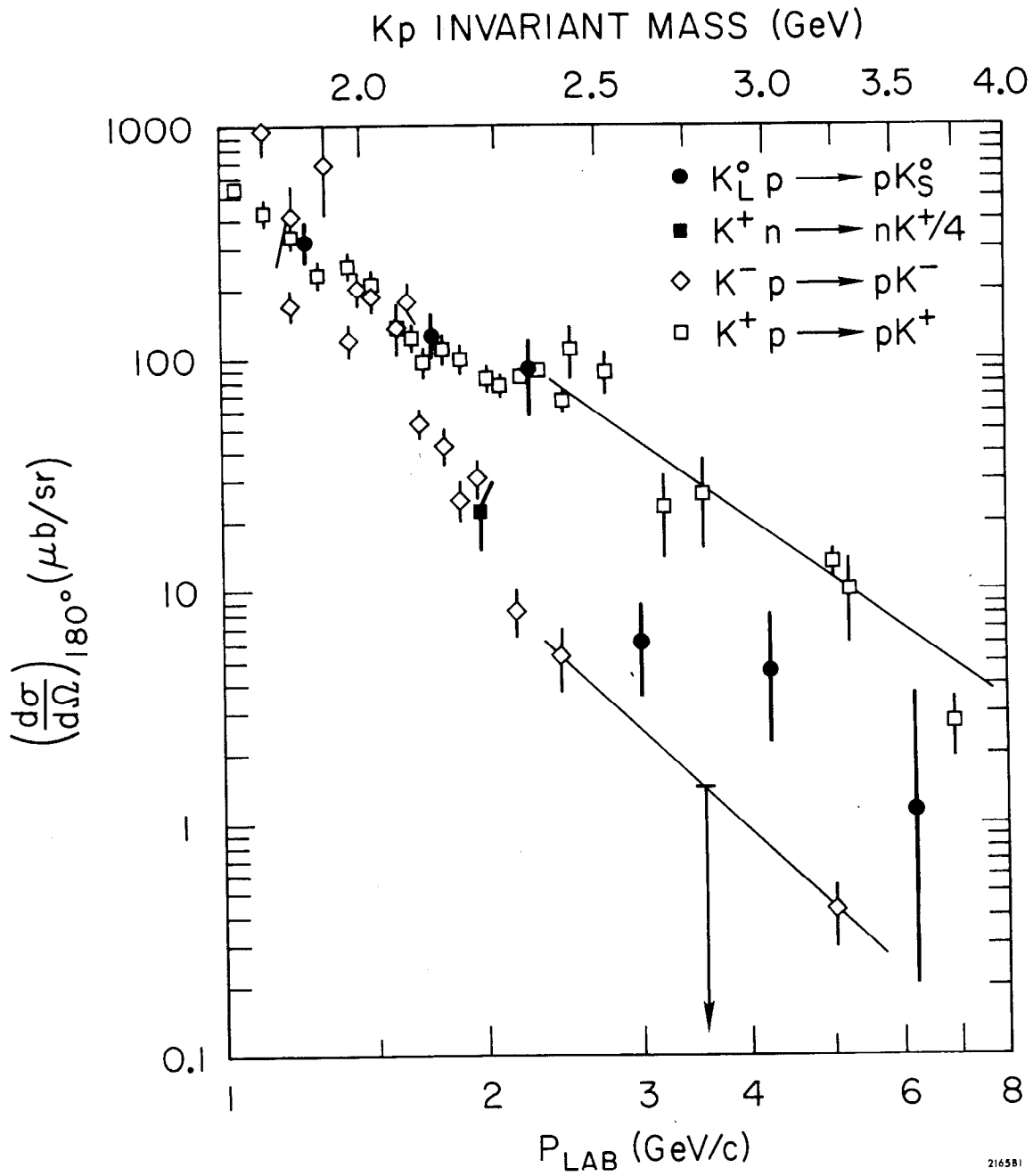


Fig. 2